Research Article ISSN Online: 2783-4859 Computational Mathematics and Computer Modeling with Applications

Received 12 March 2023
Accepted 12 April 2024

DOI: 10.48308/CMCMA.2.1.54
AMS Subject Classification: 26A33; 65L06

Three-dimensional projectile motion: analytical solution and numerical treatment of the fractional case

Nader Biranvand[a], Amir Hossein Salehi Shayegan[b] ,Hamid Ranjbar[a] and Saeed Hashemi Sababe[c]

This paper focuses on deriving analytical solutions for three-dimensional projectile motion and investigating numerical approaches for handling these solutions. We derive the equations of projectile motion using both classical and fractional calculus, considering scenarios with and without air resistance. We analyze the characteristics of the projectile's trajectory in both classical and fractional scenarios, providing a comparative study between them. Additionally, we propose an extrapolation method tailored to the nature of the motion equations to estimate projectile trajectories. The accuracy of our proposed method is assessed through the absolute error between exact and numerical solutions, with numerical examples provided to validate the theoretical analysis. Copyright © 2023 Shahid Beheshti University.

Keywords: Three-dimensional projectile motion; Fractional calculus; Caputós fractional derivative; Extrapolation method.

1. Introduction

The exploration of the motion of objects projected in two dimensions, influenced solely by gravity, constitutes one of the oldest and most frequently encountered phenomena in classical mechanics. Termed projectile motion (PM), this field, often referred to as ballistics, traces its origins back to the investigations of Galileo in the 1600s. Prior to Galileo's work, it was commonly believed that PM adhered to the theory of impetus or momentum, positing that a projectile would continue in a straight path until its momentum waned, causing it to fall directly downward. Galileo's groundbreaking studies, however, revealed that PM comprises both horizontal and vertical components, each operating independently to produce a parabolic trajectory. This seminal discovery fundamentally altered the understanding of projectile behavior and laid the groundwork for subsequent research.

Traditionally, introductory treatments of two-dimensional PM have assumed that only gravitational forces affect the projectile's motion. However, empirical evidence suggests that real-world projectiles often encounter air resistance, complicating their trajectories. Experimental observations indicate that air resistance typically manifests as a force proportional to the projectile's velocity, with variations including linear and quadratic models. Numerous scholars have tackled the analytical and numerical challenges posed by two-dimensional PM subject to linear or quadratic drag forces. For instance, Hayen [12, 13] investigated particle motion in a resistant medium under quadratic drag, devising a method that yields exact, time-implicit solutions. Morales [19] derived analytical solutions for range and optimal projectile angles in the presence of linear drag, expressed in terms of the Lambert W function. Similarly, Hu et al. [15] addressed linear resistance problems, furnishing explicit solutions for range and optimal elevation angles using the Lambert W function. The extension of Morales' work to two-dimensional PM with quadratic air resistance was later accomplished by a secondary branch of the Lambert function [19].

While classical calculus has historically sufficed for modeling two-dimensional PM, its inability to capture certain material and process properties has led researchers to explore alternatives. Fractional calculus, with its capacity to model memory-dependent phenomena, has emerged as a promising tool for achieving higher accuracy in PM analyses. Ebaid [8] extended fractional

[a] *Department of Mathematics, Faculty of Basic Science, Imam Ali University, Tehran, Iran.*
[b] *Mathematics Department, Faculty of Basic Science, Khatam-ol-Anbia (PBU) University, Tehran, Iran.*
[c] *Department of Mathematical and Statistical Sciences, University of Alberta, Edmonton, Alberta, Canada.*
[*] *Correspondence to: S.H. Sababe. Email: hashemi_1365@yahoo.com*

calculus to study two-dimensional PM in both resistive and non-resistive environments, comparing fractional PM features such as time of flight and trajectory with mortar experimental data. Ahmad et al. [1] investigated two-dimensional PM using the Riemann-Liouville derivative, contrasting trajectory features obtained via fractional Caputo derivatives. However, their approach of replacing ordinary derivatives with fractional ones lacked physical and engineering rigor.

To address this issue, Rosales Garcia et al. [16] introduced a fractional differential operator based on dimensional analysis, yielding equations for two-dimensional projectile motion in resisting media. However, their method was not applicable to non-resistive PM. Ebaid et al. [9] proposed a general method for studying two-dimensional fractional PM in both resistive and non-resistive settings, aligning results with experimental data and introducing a parameter estimation technique based on experimental input.

While extensive research has examined two-dimensional PM through classical and fractional calculus lenses, investigations into three-dimensional PM remain scarce. This paper aims to fill this gap by exploring three-dimensional PM from both classical and fractional perspectives. Building on prior work [9], we derive equations for three-dimensional PM under various air resistance scenarios, analyze projectile trajectories, and compare classical and fractional outcomes. Additionally, we employ an extrapolation method to predict three-dimensional PM trajectories.

The paper is organized as follows: Section 2 provides background on fractional derivatives and the Mittag-Leffler function. Section 3 presents analytical solutions for three-dimensional PM from classical and fractional viewpoints, alongside discussions on trajectory properties. Section 4 applies an extrapolation method to forecast three-dimensional PM trajectories. Numerical treatments and comparative analyses of classical and fractional scenarios are detailed in Section 5. Finally, concluding remarks are offered in Section 6.

2. Preliminaries

In this section, we review basic definitions of fractional derivatives and Mittag-Leffler function.

2.1. Fractional derivative

Over the last few decades, fractional calculus has become increasingly prevalent and important. It focuses on derivatives and integrals of arbitrary real or complex order, and has found significant applications in a wide range of engineering and scientific fields. Differential equations that incorporate derivatives with non-integer or fractional order have proven to be effective models for a wide range of physical phenomena. These phenomena span various fields including viscoelasticity models, fluid mechanics, advection-diffusion models, biological population models, optics, signals processing, and nuclear science, among others.

In many cases, the new fractional-order models prove to be more appropriate compared to the integer-order models. This is primarily attributed to their capacity to effectively depict the memory and hereditary characteristics observed in various materials. A basic tool for formulating phenomena involving memory effects is the FC [21, 20, 25]. For modeling three-dimensional PM in a fractional case, we can use some inequivalent fractional derivatives such as Riemann-Liouville and Caputo derivatives. The selected derivative to formulate three-dimensional PM must allow the utilization of physical and interpretable initial conditions of the underlying problem. On the other hand, we know that the Caputo derivative of a constant is zero, and so, in comparison with the classical integer case, this allows us to define suitable initial conditions for the fractional differential equations. Consequently, we will formulate in this paper the equations of PM in terms of the fractional derivative of the Caputo type. We commence from the Riemann-Liouville integral.

Definition 2.1 *The RiemannLiouville fractional integral of order γ, which is derived from Abels integral, was firstly defined by Riemann as [19]*

$$ {}_0I_t^{\gamma} f(t) = \frac{1}{\Gamma(\gamma)} \int_0^t \frac{f(\tau)}{(t-\tau)^{1-\gamma}} \mathrm{d}\tau, \tag{1} $$

where $\Gamma(.)$ denotes the Euler Gamma function.

We now define Caputo fractional derivate.

Definition 2.2 *The Caputo fractional derivative ${}_0^C D_t^{\gamma} f(t)$ of order $\gamma > 0$ is defined by [23]*

$$ {}_0^C D_t^{\gamma} f(t) = \frac{\mathrm{d}^{\gamma} f(t)}{\mathrm{d}t^{\gamma}} = \frac{1}{\Gamma(n-\gamma)} \int_0^t \frac{f^{(n)}(\tau)}{(t-\tau)^{\gamma-n+1}} \mathrm{d}\tau, \tag{2} $$

where $n \in \mathbb{N}$ and $n-1 < \gamma \leq n$.

The Laplace transform of the Caputo fractional derivative is essential for solving initial value problems, e.g. PM equation. The Laplace transform of the Caputos fractional derivative is given by

$$ L\left[{}_0^C D_t^{\gamma} f(t)\right] = s^{\gamma} F(s) - \sum_{m=0}^{n-1} s^{\gamma-m-1} f^{(n)}(0). \tag{3} $$

Remark 2.3 *Some properties of the RiemannLiouville fractional integral and the Caputo derivative are given as:*

$$\begin{aligned}
&\frac{\mathrm{d}}{\mathrm{d}t}\,{}_0I_t^{\gamma+1} = {}_0I_t^{\gamma},\\
&{}_0I_t^{\gamma}({}_0I_t^{\beta}f) = {}_0I_t^{\gamma+\beta}f,\\
&{}_0^C D_t^{\gamma}c = 0,\ (c \text{ is constant}),\\
&{}_0^C D_t^{\gamma}t^{\beta} = \frac{\Gamma(\beta+1)t^{\beta-\gamma}}{\Gamma(\beta-\gamma+1)},\ \beta>\gamma-1,\ \beta>-1,\\
&{}_0^C D_t^{\gamma}({}_0I_t^{\gamma}f(t)) = f(t)\\
&{}_0I_t^{\gamma}({}_0^C D_t^{\gamma}f(t)) = f(t) - \sum_{k=0}^{m-1} f^{(k)}(0^+)\frac{t^k}{k!},\ t>0.
\end{aligned}$$

2.2. Mittag-Leffler function

The importance of Mittag-Leffler function has been increasingly recognized in recent decades, owing to its direct relevance to the fields of physics, biology, engineering, and applied sciences. This mathematical function is named in honor of Magnus Gustaf (Gosta) Mittag-Leffler, a renowned mathematician from Sweden. This function also plays a key role in the solution of fractional order differential equations or fractional order integral equations. It serves as a direct extension of exponential functions and can be defined through a power series [14, 21, 23, 25].

Definition 2.4 *The two-parameter Mittag-Leffler function is a special function defined by*

$$\mathrm{E}_{\alpha,\beta}(z) = \sum_{m=0}^{\infty}\frac{z^m}{\Gamma(\alpha m+\beta)},\ \alpha,\beta>0,\ z\in\mathbb{C}. \tag{4}$$

When $\beta=1$, $E_{\alpha,\beta}(z)$ is abbreviated as $E_\alpha(z)$ and it is called one-parameter Mittag-Leffler function, which is a generalization of the exponential function $E_1(z)=\mathrm{e}^z$.

Humbert and Agarwal employed the Laplace transform technique to derive various relationships for this function. Despite the possibility of naming it the Agarwal function, they decided to retain the same notation as the one-parameter Mittag-Leffler function. Consequently, the two-parameter function is now commonly known as the Mittag-Leffler function. The MittagLeffler function has the following properties:

$$\begin{aligned}
&\mathrm{E}_{\alpha,\beta}(z) = \beta\mathrm{E}_{\alpha,\beta+1}(z) + \alpha z\frac{\mathrm{d}}{\mathrm{d}z}\mathrm{E}_{\alpha,\beta+1}(z),\\
&\mathrm{E}_{\alpha,\beta}(z) = \frac{1}{\Gamma(\beta)} + z\mathrm{E}_{\alpha,\alpha+\beta}(z),\\
&{}_0I_t^{\gamma}(t^{\eta-1}\mathrm{E}_{\delta,\eta}(at^{\delta})) = t^{\eta+\gamma-1}\mathrm{E}_{\delta,\eta+\gamma}(at^{\delta}),\quad \eta,\delta,\gamma>0.
\end{aligned}$$

As we already mentioned, one of the applications of the Laplace transform in science and engineering is its usefulness in solving physical problem. In solving the equations of fractional PM, we usually encounter the Laplace transform of the Mittag-Leffler function which is given by the formula

$$\int_0^{\infty}\mathrm{e}^{-st}t^{\gamma m+\beta-1}\mathrm{E}_{\alpha,\beta}^{(m)}(\pm at^{\gamma})\mathrm{d}t = \frac{m!s^{\gamma-\beta}}{(s^{\gamma}\mp a)^{m+1}}. \tag{5}$$

So, the inverse Laplace transform is given by

$$L^{-1}\left[\frac{m!s^{\gamma-\beta}}{(s^{\gamma}\mp a)^{m+1}}\right] = t^{\gamma m+\beta-1}\mathrm{E}_{\alpha,\beta}^{(m)}(\pm at^{\gamma}). \tag{6}$$

3. Three-dimensional PM: analytical solution

In this section, we obtain analytical solutions of the three-dimensional PM from classical and fractional point of view. We also study the properties of the trajectory of the motion for the cases of classical and fractional separately, and compare them with each other. We first study three-dimensional PM in classical case.

3.1. Three-dimensional classical PM

Suppose that an object with the initial velocity v_0 and mass m is projected into space under a uniform gravitational force g. We commence from the case that the effects of air resistance are assumed to be negligible. Under these conditions, the vector form of the classical equations of motion in the (x, y, z) coordinate system, is given by [10]

$$m\frac{\mathrm{d}^2\vec{r}}{\mathrm{d}t^2} = -mg\vec{k}, \tag{7}$$

with the initial conditions

$$\begin{aligned} x(0) &= 0, \quad v_{0x} = v_0 \cos\phi_0 \sin\theta_0, \\ y(0) &= 0, \quad v_{0y} = v_0 \cos\phi_0 \cos\theta_0, \\ z(0) &= 0, \quad v_{0z} = v_0 \sin\phi_0, \end{aligned}$$

where we have assumed, for the sake of simplicity, the origin of the coordinate system is the initial position of the projectile. Here, the z-axis is selected as the vertical axis of the PM (see Figure 1).

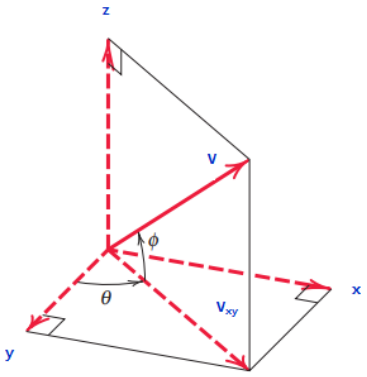

Figure 1. The components of the velocity.

In view of (7), the position vector $\vec{r}$ can be obtained by integrating both sides of (7) two times, and by using the given initial conditions as

$$\vec{r} = -\frac{1}{2}\vec{k}gt^2 + \vec{v}_0 t,$$

or, in component form,

$$\begin{aligned} x(t) &= v_{0x}t, \\ y(t) &= v_{0y}t, \\ z(t) &= v_{0z}t - \frac{1}{2}gt^2. \end{aligned} \tag{8}$$

We now turn our attention to a three-dimensional PM that the motion is subject to the force of air resistance. As we have already mentioned, the resisting force can be proportional to the projectile speed or the projectile speed squared. To compute an analytical solution for the PM, we assume that the resisting force proportional to the projectile speed. In this case, the vector representation of the equation of motion is given by [10]

$$m\frac{\mathrm{d}^2\vec{r}}{\mathrm{d}t^2} = -mg\vec{k} - mk\vec{v}, \tag{9}$$

where the components of it are given by

$$\begin{aligned} \frac{\mathrm{d}v_x}{\mathrm{d}t} &= -kv_x, \\ \frac{\mathrm{d}v_y}{\mathrm{d}t} &= -kv_y, \\ \frac{\mathrm{d}v_z}{\mathrm{d}t} &= -kv_z - g. \end{aligned} \tag{10}$$

Here $k > 0$ denotes the strength of the resistant medium, and its dimensionality is the inverse of seconds. To solve the above equation, using a technique similar to the previous case, and after performing some mathematical manipulations, we get

$$\begin{aligned} x(t) &= \frac{v_{0x}}{k}(1 - e^{-kt}), \\ y(t) &= \frac{v_{0y}}{k}(1 - e^{-kt}), \\ z(t) &= \frac{-gt}{k} + \frac{1}{k}\left(v_{0z} + \frac{g}{k}\right)(1 - e^{-kt}). \end{aligned} \tag{11}$$

The main results of equations (8) and (11) are as follows:

- In particular, if we orient the coordinate system in a such way that the x-axis lies along the projection of the initial velocity onto the xy horizontal plane, then equations (8) and (11) reduce to the solutions of classical differential equations of two-dimensional PM in the absence and in the presence of air resistance, respectively (see [9]).
- When the parameter k tends to zero, equation (11) reduce to the classical equations of three-dimensional PM (see (8)).

In the next subsection, we investigate three-dimensional PM in fractional point of view.

3.2. Three-dimensional fractional PM

To derive the equations of three-dimensional PM in the fractional case, it is necessary to substitute the ordinary derivative used in the previous case with a suitable fractional-order derivative. This fractional derivative should preserve the dimensionality of the physical quantities. Generally, authors tend to substitute integer derivative operators with fractional ones based solely on mathematical grounds. However, from an engineering standpoint, this practice is not entirely accurate, and it necessitates a dimensional correction in the new equation. In order to achieve this, Ebaid [8] proposed the idea of replacing the ordinary derivative operator $\frac{\mathrm{d}}{\mathrm{d}t}$ with a fractional-order operator $\frac{d^\beta}{dt^\beta}$, $\frac{3}{2} < \beta \leq 2$. The utilization of this technique produced incorrect values for the physical dimensions. Another method, was proposed by Rosales Garcia et al. [24], is to replace the ordinary derivative operator $\frac{\mathrm{d}}{\mathrm{d}t}$ by the fractional operator

$$\frac{\mathrm{d}}{\mathrm{d}t} \to k^{1-\gamma}\frac{\mathrm{d}^\gamma}{\mathrm{d}t^\gamma}, \ 0 < \gamma \leq 1,$$

where the auxiliary parameter k maintains the dimensionality of the physical quantities in the system and has a dimension of inverse of seconds. Their proposed scheme overcame the problem in Ebaid's strategy. Nonetheless, the procedure did not consider the comparison with the experimental findings to offer a tangible justification and can solely be employed when air resistance is factored in. To overcome this difficulty, following [24], Ebaid et al. [9] introduced the following fractional operator

$$\frac{\mathrm{d}}{\mathrm{d}t} \to \frac{1}{\sigma^{1-\gamma}}\frac{\mathrm{d}^\gamma}{\mathrm{d}t^\gamma}, \tag{12}$$

where σ is measured in seconds and is considered to have numerical values that carry physical meaning, with the possibility of experimental estimation. Using the proposed method, the authors modeled a two-dimensional PM using fractional models vis-a-vis experimental data and obtained a new solution for the equations of two-dimensional PM. Following this strategy [9], we replace $\frac{\mathrm{d}}{\mathrm{d}t}$ by $\frac{1}{\sigma^{1-\gamma}}\frac{\mathrm{d}^\gamma}{\mathrm{d}t^\gamma}$ and obtain the fractional equation of motion as

$$m\frac{\mathrm{d}^\gamma \vec{v}}{\mathrm{d}t^\gamma} = -\sigma^{1-\gamma} mg\vec{k}. \tag{13}$$

The equivalent representation of the fractional equation of motion in terms of its components is given by

$$\begin{aligned} \frac{\mathrm{d}^\gamma v_x}{\mathrm{d}t^\gamma} &= 0, \\ \frac{\mathrm{d}^\gamma v_y}{\mathrm{d}t^\gamma} &= 0, \\ \frac{\mathrm{d}^\gamma v_z}{\mathrm{d}t^\gamma} &= -\sigma^{1-\gamma} g. \end{aligned} \tag{14}$$

Now we solve the above equation using the Laplace transform. To do this, taking the Laplace transform of differential equation (14), and consequently, applying the inverse Laplace transform of both sides of the resulted differential equation, we obtain

$$\begin{aligned} v_x(t) &= \frac{\mathrm{d}x}{\mathrm{d}t} = v_{0x}, \\ v_y(t) &= \frac{\mathrm{d}y}{\mathrm{d}t} = v_{0y}, \\ v_z(t) &= \frac{\mathrm{d}z}{\mathrm{d}t} = v_{0z} - \sigma^{1-\gamma} g\frac{t^\gamma}{\Gamma(\gamma+1)}. \end{aligned} \tag{15}$$

In this position, to obtain a fractional representation of the resulting equations, we replace $v_u(t),\ u = x, y, z$ with $\frac{1}{\sigma^{1-\gamma}}\frac{\mathrm{d}^\gamma u}{\mathrm{d}t^\gamma},\ u = x, y, z$ and rewrite the (15) as

$$\begin{aligned}
\frac{\mathrm{d}^\gamma x}{\mathrm{d}t^\gamma} &= \sigma^{1-\gamma} v_{0x},\\
\frac{\mathrm{d}^\gamma y}{\mathrm{d}t^\gamma} &= \sigma^{1-\gamma} v_{0y},\\
\frac{\mathrm{d}^\gamma z}{\mathrm{d}t^\gamma} &= \sigma^{1-\gamma} v_{0z} - \sigma^{2-2\gamma} g \frac{t^\gamma}{\Gamma(\gamma+1)}.
\end{aligned} \tag{16}$$

Finally then, by taking the fractional integral ${}_0I_t^\gamma$ on both sides of equation (16), we can obtain

$$\begin{aligned}
x(t) &= \sigma^{1-\gamma} v_{0x} \frac{t^\gamma}{\Gamma(\gamma+1)},\\
y(t) &= \sigma^{1-\gamma} v_{0y} \frac{t^\gamma}{\Gamma(\gamma+1)},\\
z(t) &= \sigma^{1-\gamma} v_{0z} \frac{t^\gamma}{\Gamma(\gamma+1)} - \sigma^{2-2\gamma} g \frac{t^{2\gamma}}{\Gamma(2\gamma+1)}.
\end{aligned} \tag{17}$$

Similar to the classical case, we now study the fractional PM in the presence of air resistance. As a similar manner, which used to obtain the fractional equations of PM in the absence of air resistance, replacing $\frac{\mathrm{d}}{\mathrm{d}t}$ in equation (10) with $\frac{1}{\sigma^{1-\gamma}}\frac{\mathrm{d}^\gamma}{\mathrm{d}t^\gamma}$ implies that the fractional differential equations of PM can be written as

$$\begin{aligned}
\frac{\mathrm{d}^\gamma v_x}{\mathrm{d}t^\gamma} &= -k\sigma^{1-\gamma} v_x,\\
\frac{\mathrm{d}^\gamma v_y}{\mathrm{d}t^\gamma} &= -k\sigma^{1-\gamma} v_y,\\
\frac{\mathrm{d}^\gamma v_z}{\mathrm{d}t^\gamma} &= -k\sigma^{1-\gamma} v_z - g\sigma^{1-\gamma}.
\end{aligned} \tag{18}$$

To find the solution of this problem, we again use the Laplace transform. Taking the Laplace transform on both sides of the differential equation (18) implies that

$$\begin{aligned}
s^\gamma F_x(s) - s^{\gamma-1} v_{0x} &= -\eta F_x(s),\\
s^\gamma F_y(s) - s^{\gamma-1} v_{0y} &= -\eta F_y(s),\\
s^\gamma F_z(s) - s^{\gamma-1} v_{0z} &= -\eta F_z(s) - g\sigma^{1-\gamma},
\end{aligned} \tag{19}$$

where $\eta = k\sigma^{1-\gamma}$. Thus,

$$\begin{aligned}
v_x(t) &= L^{-1}[F_x(s)] = v_{0x} \mathrm{E}_{\gamma,1}\left(-\eta t^\gamma\right),\\
v_y(t) &= L^{-1}[F_y(s)] = v_{0y} \mathrm{E}_{\gamma,1}\left(-\eta t^\gamma\right),\\
v_z(t) &= L^{-1}[F_z(s)] = \left(v_{0z} + \frac{g}{k}\right) \mathrm{E}_{\gamma,1}\left(-\eta t^\gamma\right) - \frac{g}{k},
\end{aligned} \tag{20}$$

or, in fractional form,

$$\begin{aligned}
\frac{\mathrm{d}^{\mathrm{fl}} x}{\mathrm{d}t^\gamma} &= \sigma^{1-\gamma} v_{0x} \mathrm{E}_{\gamma,1}\left(-\eta t^\gamma\right),\\
\frac{\mathrm{d}^{\mathrm{fl}} y}{\mathrm{d}t^\gamma} &= \sigma^{1-\gamma} v_{0y} \mathrm{E}_{\gamma,1}\left(-\eta t^\gamma\right),\\
\frac{\mathrm{d}^{\mathrm{fl}} z}{\mathrm{d}t^\gamma} &= \sigma^{1-\gamma} \left(v_{0z} + \frac{g}{k}\right) \mathrm{E}_{\gamma,1}\left(-\eta t^\gamma\right) - \frac{g}{k}.
\end{aligned} \tag{21}$$

And finally, applying the fractional integral ${}_0I_t^\gamma$ and using the properties of RiemannLiouville fractional integral and MittagLeffler function yields

$$\begin{aligned}
x(t) &= \frac{\sigma^{1-\gamma} v_{0x}}{\eta}\left[1 - \mathrm{E}_\gamma\left(-\eta t^\gamma\right)\right],\\
y(t) &= \frac{\sigma^{1-\gamma} v_{0y}}{\eta}\left[1 - \mathrm{E}_\gamma\left(-\eta t^\gamma\right)\right],\\
z(t) &= \frac{-g\eta}{k^2\Gamma(\gamma+1)} t^\gamma + \frac{1}{k}\left(\frac{g}{k} + v_{0z}\right)\left[1 - \mathrm{E}_\gamma(-\eta t^\gamma)\right].
\end{aligned} \tag{22}$$

Similar to the previous case, the main observations about the fractional equations (17) and (22) are as follows:

- Similar to the classical case, if we orient the coordinate system such that the x-axis lies along the projection of the initial velocity onto the xy horizontal plane, then equations (17) and (22) reduce to the solutions of fractional differential equations of two-dimensional PM in the absence and in the presence of air resistance, respectively (see [9]).
- The analytical solutions of classical PM in the absence and in the presence of air resistance can be deduced from equations (17) and (22) at $\gamma = 1$, respectively (see (8) and (11)).
- As $k \to 0$, equation (22) reduce to the fractional equations of PM (see (11)).

3.3. The classical and fractional trajectory of PM: analytical comparison

To analyze the trajectory of a PM, three quantities should be studied; range, maximum altitude and time of flight. Since these quantities for the classical case can be deduced from fractional case at $\gamma = 1$, we only obtain these quantities for the fractional case. We first consider the fractional PM in the absence of air resistance.

Let R_F denote the range of the fractional PM. To calculate R_F, we need to obtain the fractional time of flight T_F. The total time T_F can be obtained by setting $z = 0$ in the last of equation (17), which implies that

$$T_F = \left[\frac{\Gamma(2\gamma+1)v_{0z}}{\Gamma(\gamma+1)\sigma^{1-\gamma}}\right]^{\frac{1}{\gamma}}.$$

By substituting T_F into the first and the second equation of (17), we obtain

$$R_F = \sqrt{x^2(T_F)+y^2(T_F)} = \frac{\sigma^{1-\gamma}T_F^{\gamma}v_0\cos\phi_0}{\Gamma(\gamma+1)} = \frac{v_0^2\sin(2\phi_0)\Gamma(2\gamma+1)}{2g(\Gamma(\gamma+1))^2}. \tag{23}$$

The range of the classical PM R_C can be obtained from the fractional range R_F at $\gamma = 1$, i.e.,

$$R_C = \frac{v_0^2\sin(2\phi_0)}{g}. \tag{24}$$

As we see, R_F has its maximum value $R_{F-\max} = \dfrac{v_0^2\Gamma(2\gamma+1)}{2g(\Gamma(\gamma+1))^2}$, which corresponds to $2\phi_0 = \dfrac{\pi}{4}$ or $\phi_0 = \dfrac{\pi}{2}$. It also implies that $R_{C-\max} = \dfrac{v_0^2}{g}$.

We now calculate the maximum height of the fractional PM. As we know, at maximum height the z-axis velocity component is zero. Therefore, by setting $v_z = 0$ in the last of equation (15) and solving for t, we obtain

$$T_{\text{maximum height}} := T_{H-max} = \left[\frac{v_{0z}\Gamma(\gamma+1)}{\sigma^{1-\gamma}g}\right]^{\frac{1}{\gamma}}.$$

Therefore, by putting T_{H-max} into the third equation of (17), we obtain the fractional maximum height $H_{F-\max}$ as

$$H_{F-\max} = \frac{v_{0z}^2}{g}\left(1 - \frac{(\Gamma(\gamma+1))^2}{\Gamma(2\gamma+1)}\right). \tag{25}$$

As $\gamma \to 1$, we recover the classical case and obtain the maximum height $H_{C-\max}$ as

$$H_{C-\max} = \frac{v_0^2\sin^2\phi_0}{2g}. \tag{26}$$

The above argument leads to the following lemmas which compare the range and the maximum height of PM for classical and fractional cases.

Lemma 3.1 *Assume that R_F and R_C denote the range of PM in fractional and classical cases, respectively. Then the relation between R_F and R_C is given by*

$$\rho(\gamma) := \frac{R_F}{R_C} = \frac{\Gamma(2\gamma+1)}{2(\Gamma(\gamma+1))^2},$$

hence the range of PM in fractional case at different values of γ is always less than the range of PM in classical case.

Proof. Using R_F and R_C, we obtain

$$\rho(\gamma) = \frac{R_F}{R_C} = \frac{\Gamma(2\gamma+1)}{2(\Gamma(\gamma+1))^2}.$$

Since the function $\rho(\gamma)$ is strictly increasing on $(0, 1]$, so it attains its maximum value at $\gamma = 1$ (see Figure 2). This completes the proof of the lemma. □

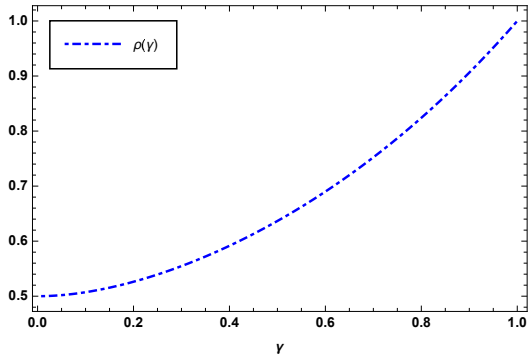

Figure 2. Graph of the function $\rho(\gamma)$ for different values of $0 < \gamma \leq 1$.

Lemma 3.2 *Assume that $H_{F-\max}$ and $H_{C-\max}$ denote the maximum height of PM in fractional and classical cases, respectively. Then the relation between $H_{F-\max}$ and $H_{C-\max}$ is given by*

$$\delta(\gamma) := \frac{H_{F-\max}}{H_{C-\max}} = \frac{2(\Gamma(2\gamma+1) - \Gamma(\gamma+1)^2)}{\Gamma(2\gamma+1)},$$

hence the the maximum height of PM in fractional case at different values of γ is always less than the the maximum height of PM in classical case.

Proof. Using $H_{F-\max}$ and $H_{C-\max}$, we obtain

$$\delta(\gamma) = \frac{H_{F-\max}}{H_{C-\max}} = \frac{2(\Gamma(2\gamma+1) - \Gamma(\gamma+1)^2)}{\Gamma(2\gamma+1)}.$$

As we see the function $\delta(\gamma)$ is strictly increasing on $(0, 1]$, and therefore, it attains its maximum value at $\gamma = 1$ (see Figure 3). This completes the proof of the lemma. □

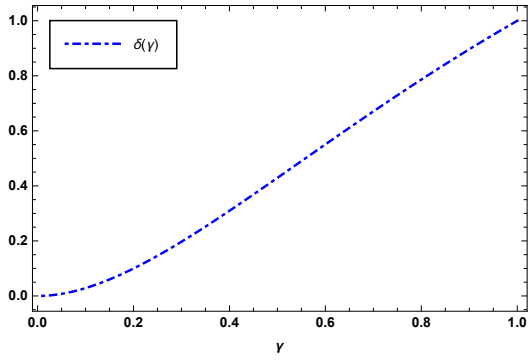

Figure 3. Graph of the function $\delta(\gamma)$ for different values of $0 < \gamma \leq 1$.

We now concentrate on the trajectory of fractional PM in the presence of air resistance. To find the range of the fractional PM R_F, similar to the previous case, we first need to compute the fractional time of flight T_F. From (22) we have to solve the following equation in T_F:

$$\frac{g\eta}{k^2\Gamma(\gamma+1)} T_F^\gamma = \frac{1}{k}\left(\frac{g}{k} + v_{0z}\right)\left[1 - \mathrm{E}_\gamma(-\eta T_F^\gamma)\right]. \tag{27}$$

As we see (27) is a transcendental equation and needs to be solved by some numerical methods since it has no explicit solution for T_F. In order to compute T_F, we can truncate the series

$$\mathrm{E}_\gamma(-\eta T_F^\gamma) = \sum_{m=0}^{\infty} \frac{(-\eta T_F^\gamma)^m}{\Gamma(\alpha m+1)},$$

and solve numerically the following equation

$$\frac{g\eta}{k^2\Gamma(\gamma+1)} T_F^\gamma = \frac{1}{k}\left(\frac{g}{k} + v_{0z}\right)\left[1 - \sum_{m=0}^{N} \frac{(-\eta T_F^\gamma)^m}{\Gamma(\alpha m+1)}\right]. \tag{28}$$

To solve the above equation, we can use some well-known numerical methods such as the Broyden method, the steepest descent method, the Newton method or a mathematical software package. In this paper, we have used Mathematicas routine FindRoot. This routine can perform this task provided that at least an initial guess of the solution of the underlying equation is known. On the other hand, the solution is very sensitive to the initial guess, and this routine may fail to converge to the desired solution whenever the starting point is selected badly. In this and forthcoming transcendental equations, an initial point is selected by the steepest descent method [7]. After solving this equation, the range of the fractional PM R_F can be obtained by substituting T_F into the first and the second equation of (22), which implies that

$$R_F = \sqrt{x^2(T_F) + y^2(T_F)} = \frac{g\sigma^{1-\gamma} T_F^{\gamma} v_0 \cos\phi_0}{\Gamma(\gamma+1)(g + k v_0 \sin\phi_0)}. \tag{29}$$

Similarly, to obtain the maximum height of the fractional PM in the presence of air resistance, we first need to find the solution of the following transcendental equation

$$\left(v_{0z} + \frac{g}{k}\right) \mathrm{E}_{\gamma,1}\left(-\eta H_{F-\max}^{\gamma}\right) = \frac{g}{k}, \tag{30}$$

which can be solved again by Mathematicas routine FindRoot. To derive the solution of the above equation, similar to (28), we can truncate the series

$$\mathrm{E}_{\gamma}(-\eta H_{F-\max}^{\gamma}) = \sum_{m=0}^{\infty} \frac{(-\eta H_{F-\max}^{\gamma})^m}{\Gamma(\alpha m+1)},$$

and obtain the numerical solution of the following equation

$$\left(v_{0z} + \frac{g}{k}\right) \left[\sum_{m=0}^{N} \frac{(-\eta H_{F-\max}^{\gamma})^m}{\Gamma(\alpha m+1)}\right] = \frac{g}{k}. \tag{31}$$

Unlike the previous case, the above argument implies that the comparison between the range and the maximum height of classical and fractional PM in the presence of air resistance is only possible by numerical comparison, which we will do in section 5.

4. Prediction of three-dimensional PM trajectory

In this section we try to predict the trajectory of three-dimensional PM by extrapolation method. We confirm the obtained results by numerical examples in the next section.

One of the methods to predict the value of an unknown variable based on the observation of other data points is the extrapolation method. There are three types of the extrapolation method; linear, conic, and polynomial extrapolation. We review these methods, briefly[7]:

- **Linear extrapolation.** When we want to predict the value which is not too far beyond the existing data or extend an approximately linear function away from its domain, linear extrapolation can be provide good results. Assume that two endpoints (x_{k-1}, y_{k-1}) and (x_k, y_k) are nearest the point $\bar{x}$, then the extrapolation formula is given by

$$P(\bar{x}) = y_{k-1} + (\bar{x} - x_{k-1}) \left(\frac{y_{k-1} - y_k}{x_{k-1} - x_k}\right). \tag{32}$$

- **Cubic extrapolation.** In this type of extrapolation, we create a conic section with the help of the last five endpoints of the known data. In this method, the obtained extrapolation may be curve back on itself if the conic section created is a circle or ellipse. But when we have a parabola or hyperbola, the curve may be relative to the x-axis and consequently, it will not back on itself.
- **Polynomial extrapolation.** In this case, we make a polynomial curve that uses all the known data points or just the endpoints. The mentioned curve is usually constructed by Lagrange's interpolation or Newtons system of finite series. The obtained polynomial is applied to extrapolate the data using the associated endpoints.

As we see, the aforementioned extrapolation methods use a polynomial interpolation to estimate the trajectory of a PM. Therefore, to analyze the error of the proposed method, we have to investigate the error of the polynomial interpolation. Assume that $x_0, x_1, \ldots, x_n$ are distinct points within the interval $[a, b]$ and $P_n(x)$ denotes the interpolating polynomial of the function $f \in C^n[a, b]$ at mentioned points. Then, for any $x \in [a, b]$, there exists $\xi = \xi(x)$ in (a, b) such that [7]

$$f(x) - P_n(x) = \frac{(x - x_0)(x - x_1)\ldots(x - x_n)}{(n+1)!} f^{(n)}(\xi).$$

The above error formula implies that, for a smooth function f, the distance between x and interpolation points x_i, $i = 0, 1, \ldots, n$, i.e., the value of the term $(x - x_0)(x - x_1)\ldots(x - x_n)$, has main contribution to the size of the error of the proposed

extrapolation method. Therefore, to control the impact of this term in the whole error, we have to predict the trajectory of the projectile using a few endpoints of the known data, since the value of $(x - x_i)$, $i = 0, 1, \ldots, n$ has the minimum value in this case.

Remark 4.1 *The quality of an extrapolation method depends strongly on the assumptions about the function made by the method. For example, if we let the known data are smooth, then the method poorly extrapolates a non-smooth function. Therefore, the proposed method should be used with caution. However, in this paper, the equations of PM are known, and therefore, the existing data for extrapolation are extracted from these equations. This means that we can use appropriate extrapolation to predict an unknown value of given data beyond its range.*

5. Numerical results and discussions

In this section we provide some numerical experiments which confirm the theoretical results of the paper. Before presenting the numerical examples, we have to estimate the values of the parameters σ, γ and k using the available experimental data of a real-world projectile.

For a two-dimensional PM in the absence of air resistance, Ebaid et al. [9] obtained the relation between σ and γ using experimental data. They also found a relation between σ and the resistant parameter k in the presence of air resistance. In the absence of air resistance, the authors computed σ vs γ for 4 different values of the initial velocity v_0 of a mortar and $\gamma \in (0, 1]$. They found that choosing $\sigma = 4.12295$ vs $\gamma = 0.92$ improve the results of fractional calculus in view of the experimental data. In the presence of air resistance, they studied the variation of σ versus k for $\sigma = 0.92$. They found that k shold belongs to the interval $[0, 0.0025]$, which implies that choosing $\sigma = 0.92$ and $k = 0.0025$ lead to the average value $\sigma = 4.34416$. For estimating these parameters in a three-dimensional PM, using (23) and (29), we have to utilize the following expressions

$$\sigma = \left(\frac{\Gamma(\gamma + 1) R_F}{T_F^{\gamma} v_0 \cos \phi_0} \right)^{\frac{1}{1-\gamma}}, \tag{33}$$

$$\sigma = \left(\frac{\Gamma(\gamma + 1) R_F (k v_0 \sin \phi_0 + g)}{T_F^{\gamma} v_0 \cos \phi_0} \right)^{\frac{1}{1-\gamma}}. \tag{34}$$

in the absence and in the presence of stationary points, respectively. These relations for a three-dimensional PM are equal to the ones obtained for a two-dimensional PM (see [9]). Therefore, we can use the aforementioned values of the parameters σ, γ and k in the following examples, which are extracted using fractional models of a two-dimensional PM vis-a-vis experimental data.

We first compare the properties of the classical and fractional three-dimensional PM and confirm the expected results of Lemmas 1 and 2.

Example 5.1 *Let an object is projected from the origin with speed $v_0 = 131.36$ m/s and launch angles $\phi_0 = \frac{\pi}{4}$, $\theta_0 = \frac{\pi}{3}$. We first compare the range and the maximum height of classical and fractional PM in the absence of air resistance. Using (33), we select $\sigma = 4.12295$ s and plot the trajectory of three-dimensional PM for different values of γ in Figure 4. We observe that the range of fractional PM for different values of γ is always less than the range of classical PM, which confirms the theoretical results of Lemma 3.1.*

Moreover, we plot the maximum height of PM for classical and fractional cases in Figure 5. We see that the maximum height of fractional PM for different values of γ is always less than the maximum height of classical PM. This confirms the results of Lemma 3.2.

We now concentrate on comparing the range and the maximum height of classical and fractional PM in the presence of air resistance. Using (34), we select $k = 0.0005$ s^{-1}, $\sigma = 4.34416$ s, solve equations (28) and (31) and use them to obtain the range of PM in classical and fractional cases, respectively. In Figure 6, we plot the trajectory of tree-dimensional PM for different values of γ. Similar results have been observed for this case; the range of fractional PM for different values of γ is always less than the range of classical PM.

Furthermore, similar to previous case, we plot in Figure 7 the maximum height of PM for classical and fractional cases. The message is the same as the previous case: the maximum height of fractional PM for different values of γ is always less than the maximum height of classical PM.

In [9] it was observed that the results of the range R_F and the flight time T_F of a two-dimensional fractional PM, in comparison with two-dimensional classical PM, are close to the experimental data of one mortar collected by the American Ministry of Defense [17]. Since the range and the flight time of a three-dimensional PM are equal to the ones established for a PM in two dimensions, the aforementioned result is also true for a PM in three dimensions.

Now, we illustrate the efficiency and accuracy of the proposed extrapolation method which applied to prediction of three-dimensional projectile trajectories.

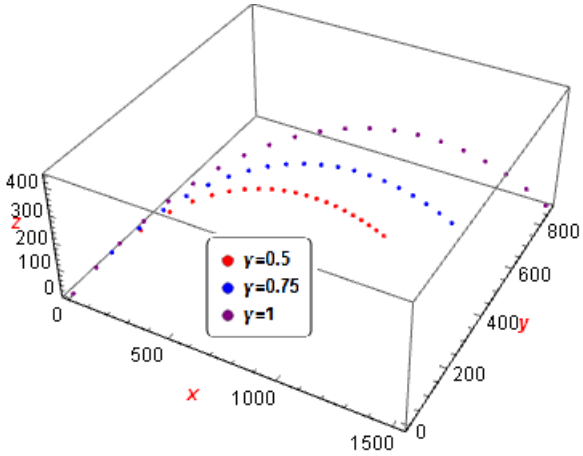

Figure 4. Comparing the range of classical and fractional three-dimensional PM for $v_0 = 131.36\ m/s$, $\phi_0 = \frac{\pi}{4}$, $\theta_0 = \frac{\pi}{3}$, $g = 9.81\ m/s^2$ and different values of γ.

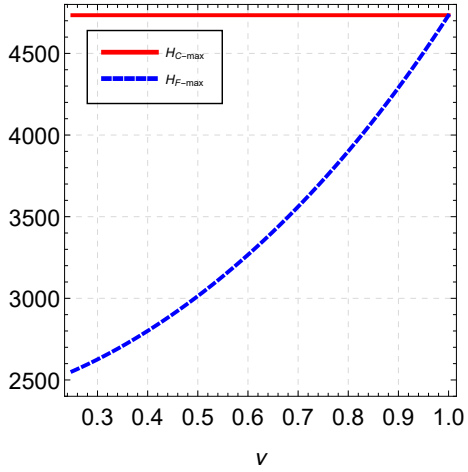

Figure 5. Comparing the maximum height of classical and fractional three-dimensional PM for $v_0 = 131.36\ m/s$, $\phi_0 = \frac{\pi}{4}$, $\theta_0 = \frac{\pi}{3}$, $g = 9.81\ m/s^2$ and different values of γ.

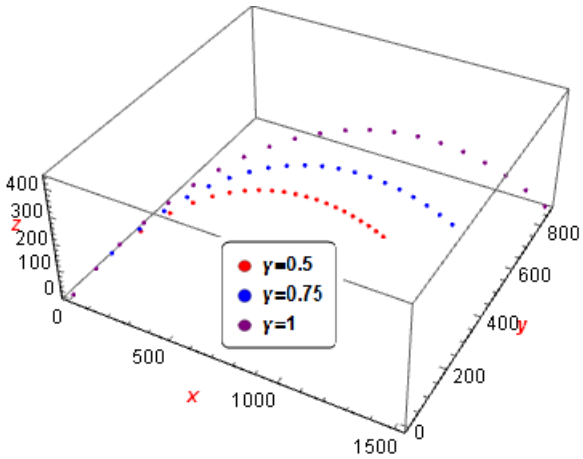

Figure 6. Comparing the range of classical and fractional three-dimensional PM for $v_0 = 131.36\ m/s$, $\phi_0 = \frac{\pi}{4}$, $\theta_0 = \frac{\pi}{3}$, $g = 9.81\ m/s^2$ and different values of γ.

Example 5.2 *Assume that an object with initial velocity $v_0 = 131.36\ m/s$ and launch angles $\phi_0 = \frac{\pi}{4}$, $\theta_0 = \frac{\pi}{3}$ is projected into a spatial which is subjected to a uniform gravitational field. We commence from the case in which any other forces such as air*

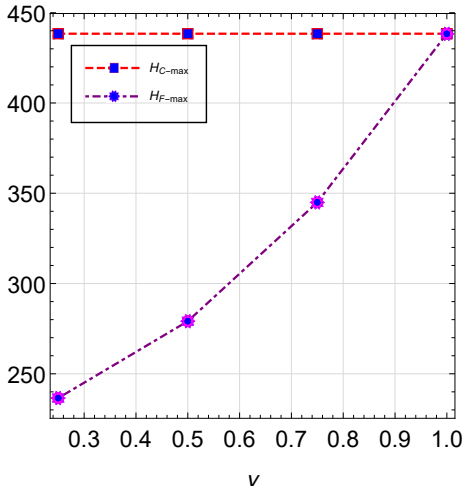

Figure 7. Comparing the maximum height of classical and fractional three-dimensional PM for $v_0 = 131.36\ m/s,\ \phi_0 = \frac{\pi}{4},\ \theta_0 = \frac{\pi}{3},\ g = 9.81\ m/s^2$ and different values of γ.

resistance are neglected. Using the classical equations of motion (8), in Figure 8 we display the trajectory of the projectile for $g = 9.81\ m/s^2$ and $t \in [0, t_C]$ where t_C denotes the classical time of flight.

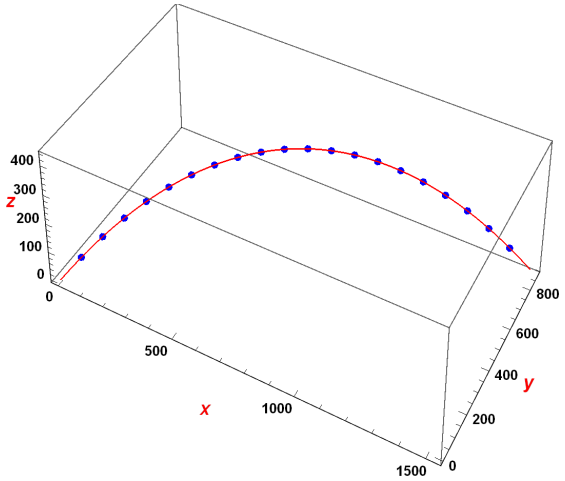

Figure 8. The trajectory of classical PM for $v_0 = 131.36\ m/s,\ \phi_0 = \frac{\pi}{4},\ \theta_0 = \frac{\pi}{3}$ and $g = 9.81\ m/s^2$.

Since the equations of motion in classical case are polynomials of degree at most two, we predict its trajectory by quadratic polynomial extrapolation. For this, let

$$I_h := \left\{ t_j : t_j = jh,\ j = 0,\ 1,\ \ldots,\ N = \frac{t_C}{h} \right\},$$

be a uniform grid on $[0, t_C]$ where $t_C = 18.9369\ s$ and $N = 12$. For each interval $[t_{k-1}, t_{k+1}],\ k = 1, 2, \ldots, 10$, we construct a quadratic interpolation function $P_2(t)$ which approximate each equation of PM (8) and then, predict the trajectory of PM at time $t_{k+2},\ k = 2, 3, \ldots, 10$. The absolute errors for each t_{k+2} are displayed in Table 1.

Figure 9 shows graphically the results obtained in Table 1. This figure and Table 1 share the same message: the proposed extrapolation rule efficiently predicts the trajectory of the three-dimensional PM.

We now consider the mentioned three-dimensional PM in view of FC. The trajectory of PM for $v_0 = 131.36\ m/s,\ \phi_0 = \frac{\pi}{4},\ \theta_0 = \frac{\pi}{3},\ \sigma = 4.12295\ s,\ \gamma = 0.92$ and $g = 9.81\ m/s^2$ is displayed in Figure 10.

In this case, the fractional equations of PM (17) are functions of the form $t^\beta,\ 0 < \beta \leq 2$. To obtain accurate numerical results, we estimate the trajectory of motion by polynomial extrapolation based on the six point of each interval $[t_k, t_{k+5}],\ k = 15, 17, \ldots, 24$ such that the points t_k are belong to the uniform grid

$$I_h = \left\{ t_j : t_j = jh,\ j = 0,\ 1,\ \ldots,\ N = \frac{t_F}{h} \right\},$$

Table 1. The absolute errors of the prediction of three-dimensional classical PM trajectory at time t_{k+2}, $k = 2, 3, \ldots, 10$.

t_i	Error at x-axis	Error at y-axis	Error at z-axis
t_3	0	0	2.8000×10^{-14}
t_4	0	0	1.4000×10^{-13}
t_5	5.7000×10^{-14}	5.7000×10^{-14}	2.2700×10^{-13}
$\vdots$	$\vdots$	$\vdots$	$\vdots$
t_{10}	6.8200×10^{-13}	1.2510×10^{-12}	4.5500×10^{-13}
t_{11}	1.3640×10^{-12}	4.5500×10^{-13}	1.8190×10^{-12}
t_{12}	1.3640×10^{-12}	3.4500×10^{-13}	4.5500×10^{-13}

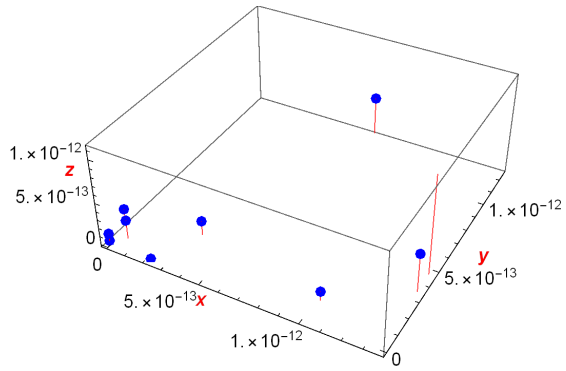

Figure 9. The absolute errors for $v_0 = 131.36\ m/s$, $\phi_0 = \frac{\pi}{4}$, $\theta_0 = \frac{\pi}{3}$ and $g = 9.81\ m/s^2$.

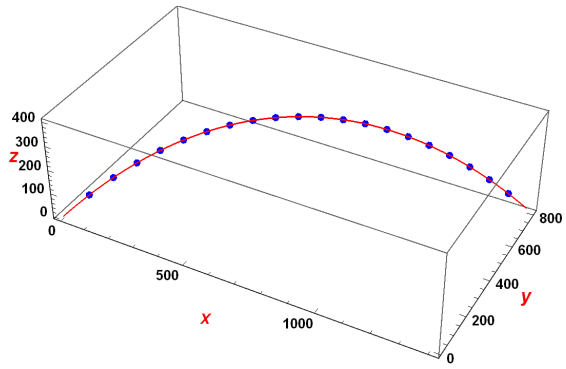

Figure 10. The trajectory of fractional PM for $v_0 = 131.36\ m/s$, $\phi_0 = \frac{\pi}{4}$, $\theta_0 = \frac{\pi}{3}$, $\sigma = 4.12295\ s$, $\gamma = 0.92$ and $g = 9.81\ m/s^2$.

and $t_F = 19.169\ s$, $N = 30$. *Therefore, we predict the trajectory of PM at time* t_{k+6}, $k = 15, 16, \ldots, 24$ *and list the absolute errors for each point in Table 2.*

Table 2. The absolute errors of the prediction of three-dimensional fractional PM trajectory at time t_{k+6}, $k = 15, 16, \ldots, 24$.

t_i	Error at x-axis	Error at y-axis	Error at z-axis
t_{15}	7.3811×10^{-5}	4.2615×10^{-5}	1.3247×10^{-4}
t_{16}	5.5048×10^{-5}	3.1782×10^{-5}	1.0073×10^{-4}
t_{17}	4.1724×10^{-5}	2.4089×10^{-5}	7.7808×10^{-5}
$\vdots$	$\vdots$	$\vdots$	$\vdots$
t_{28}	1.2632×10^{-5}	7.2930×10^{-6}	2.5735×10^{-5}
t_{29}	1.0255×10^{-6}	5.9208×10^{-5}	2.1242×10^{-5}
t_{30}	8.3947×10^{-6}	4.8467×10^{-6}	1.7674×10^{-5}

Furthermore, like Figure 9, we display in Figure 11 the absolute errors achieved in Table 2. The results indicate that the proposed method efficiently and accurately predicts the trajectory of PM.

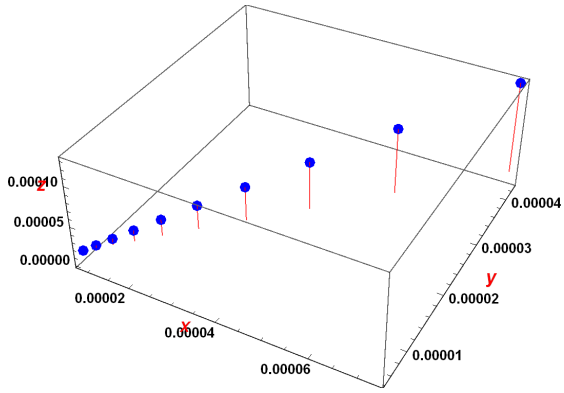

Figure 11. The absolute errors for $v_0 = 131.36\ m/s,\ \phi_0 = \frac{\pi}{4},\ \theta_0 = \frac{\pi}{3},\ \sigma = 4.12295\ s,\ \gamma = 0.92$ and $g = 9.81\ m/s^2$.

We now implement the proposed method to predict the trajectory of the PM in the case that the motion is subject to the force of air resistance. Similar to the previous case, we first study three-dimensional PM in view of classical calculus. For an object which is projected into a spatial with initial velocity $v_0 = 131.36\ m/s$ and launch angles $\phi_0 = \frac{\pi}{4},\ \theta_0 = \frac{\pi}{3}$, let the strength of the retarding force k is equal to $0.0005\ s^{-1}$. We use the classical equations of motion (11) and plot in Figure 12 the trajectory of PM for $g = 9.81\ m/s^2$ and $t \in [0, t_C]$ where t_C again denotes the classical time of flight.

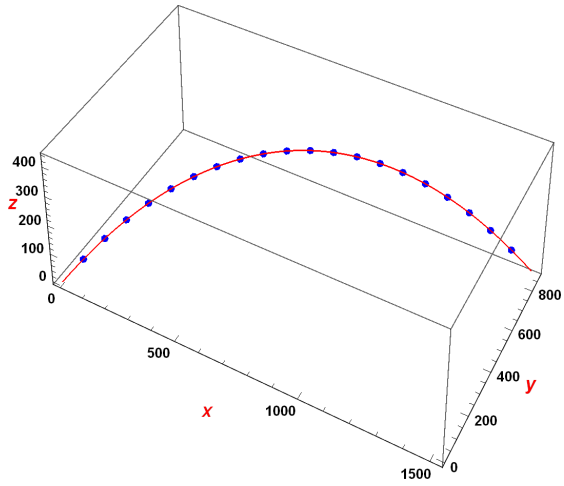

Figure 12. The trajectory of classical PM for $v_0 = 131.36\ m/s,\ \phi_0 = \frac{\pi}{4},\ \theta_0 = \frac{\pi}{3},\ k = 0.0025\ s^{-1}$ and $g = 9.81\ m/s^2$.

As we see the equations of motion are in terms of the exponential function. Therefore, to obtain an accurate approximation of the projectile trajectory, we use a polynomial extrapolation on each interval $[t_k, t_{k+5}],\ k = 15, 17, \ldots, 24$ and predict the trajectory of PM at time $t_{k+6},\ k = 15, 16, \ldots, 24$ where

$$I_h = \left\{ t_j : t_j = jh,\ j = 0,\ 1,\ \ldots,\ N = \frac{t_{C-flight}}{h} \right\},$$

and $t_C = 18.7898\ s,\ N = 30$. The absolute errors are displayed in Table 3. We also depict the obtained errors in Figure 13.

From Table 3 and Figure 13, we can see that the proposed extrapolation method accurately predict the trajectory of the PM.

In view of FC, the equations of PM are given by (22). In this case, we again assume that an object is projected into a spatial with initial velocity $v_0 = 131.36\ m/s$ and launch angles $\phi_0 = \frac{\pi}{4},\ \theta_0 = \frac{\pi}{3}$ where $k = 0.0005\ s^{-1},\ \sigma = 4.34416\ s$ and $\gamma = 0.92$. This motion is displayed in Figure 14.

In fractional case, the equations of PM are expressed in terms of MittagLeffler function. Similar to the classical case, we use a polynomial extrapolation on each interval $[t_k, t_{k+5}],\ k = 15, 17, \ldots, 24$ and predict the trajectory of PM at time $t_{k+6},\ k = 15, 16, \ldots, 24$ where

$$I_h = \left\{ t_j : t_j = jh,\ j = 0,\ 1,\ \ldots,\ N = \frac{t_F}{h} \right\},$$

Table 3. The absolute errors of the prediction of three-dimensional classical PM trajectory at time t_{k+2}, $k = 2, 3, \ldots, 10$ in the presence of air resistance.

t_i	Error at x-axis	Error at y-axis	Error at z-axis
t_{15}	0	0	1.3824×10^{-10}
t_{16}	0	0	2.0373×10^{-10}
t_{17}	0	0	2.0373×10^{-10}
$\vdots$	$\vdots$	$\vdots$	$\vdots$
t_{28}	0	0	2.5466×10^{-10}
t_{29}	0	0	2.1828×10^{-10}
t_{30}	0	0	1.8190×10^{-10}

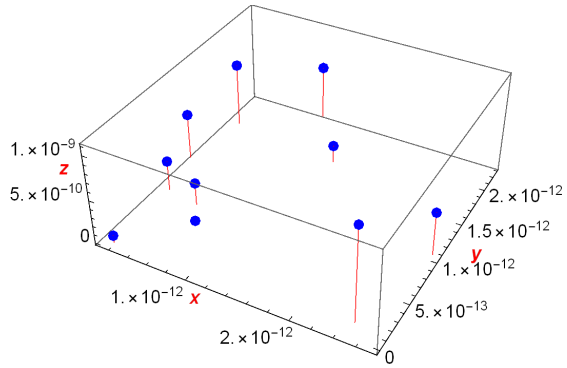

Figure 13. The absolute errors for $v_0 = 131.36\ m/s$, $\phi_0 = \frac{\pi}{4}$, $\theta_0 = \frac{\pi}{3}$, $k = 0.0025\ s^{-1}$, $\sigma = 4.12295\ s$, $\gamma = 0.92$ and $g = 9.81\ m/s^2$.

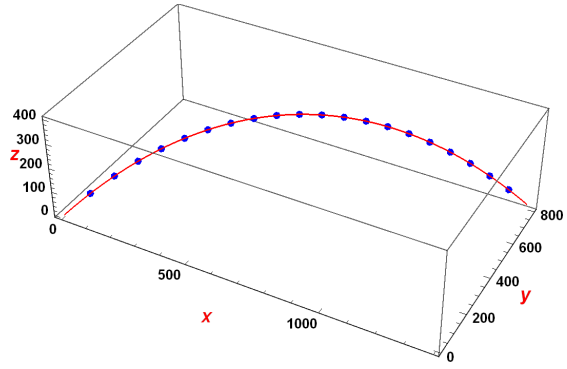

Figure 14. The trajectory of fractional PM for $v_0 = 131.36\ m/s$, $\phi_0 = \frac{\pi}{4}$, $\theta_0 = \frac{\pi}{3}$, $k = 0.0025\ s^{-1}$, $\sigma = 4.34416\ s$, $\gamma = 0.92$ and $g = 9.81\ m/s^2$.

and $t_F = 18.9340\ s$, $N = 30$. *The absolute errors and graphical presentation of these information are displayed in Table 4 and Figure 15, respectively. These results again show the efficiency and accuracy of the proposed method.*

6. Conclusion

In this paper, we obtained classical and fractional differential equations of three-dimensional PM. We studied the motion in the presence and in the absence of air resistance separately. In addition, we studied the properties of the trajectory of classical and fractional PM and compared them analytically. Then, we applied the extrapolation method to predict the trajectories of three-dimensional PM from a numerical point of view. The efficiency and accuracy of the numerical schemes were confirmed through numerical examples. The main results of the paper are as follows:

- The range and the maximum height of a three-dimensional fractional PM at different values of γ are always less than of a three-dimensional classical PM.

Table 4. The absolute errors of the prediction of three-dimensional fractional PM trajectory at time t_{k+6}, $k = 15, 16, \ldots, 24$.

t_i	Error at x-axis	Error at y-axis	Error at z-axis
t_{15}	7.4251×10^{-5}	4.2869×10^{-5}	1.3288×10^{-4}
t_{16}	5.5416×10^{-5}	3.1994×10^{-5}	1.0110×10^{-4}
t_{17}	4.2033×10^{-5}	2.4268×10^{-5}	7.8144×10^{-5}
$\vdots$	$\vdots$	$\vdots$	$\vdots$
t_{28}	1.2771×10^{-5}	7.3731×10^{-6}	2.5920×10^{-5}
t_{29}	1.0375×10^{-6}	5.9902×10^{-5}	2.1413×10^{-5}
t_{30}	8.4990×10^{-6}	4.9069×10^{-6}	1.7825×10^{-5}

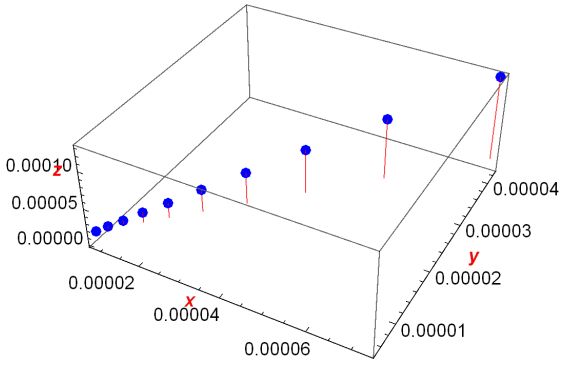

Figure 15. The absolute errors for $v_0 = 131.36\ m/s$, $\phi_0 = \frac{\pi}{4}$, $\theta_0 = \frac{\pi}{3}$, $\sigma = 4.34416\ s$, $\gamma = 0.92$ and $g = 9.81\ m/s^2$.

- The properties of the trajectory of a three-dimensional fractional PM, especially in the presence of air resistance, are close to the experimental data.
- The proposed extrapolation method efficiently estimates the trajectory of the three-dimensional PM.

It is important to note that our proposed method faces a limitation in that it is impossible to compute explicit solutions for the range and maximum height of fractional PM when air resistance is taken into account. However, we are committed to addressing this limitation in our future work. Our upcoming research will involve developing alternative models of fractional PM in the presence of air resistance, where the equations for range and maximum height can be solved analytically. Furthermore, we will also explore the option of presenting additional numerical methods to solve these equations.

References

1. B. Ahmad, H. Batarfi, Juan J. Nieto, O. Otero-Zarraquios and W. Shammakh. Projectile motion via Riemann-Liouville calculus, *Advances in Difference Equations*, 41:373–378, 2015.
2. F. M. Alharbi, D. Baleanu, A. Ebaid. Physical properties of the projectile motion using the conformable derivative, *Chinese Journal of Physics*, 58:18–28, 2019.
3. C. Hadj Belgacem. Range and flight time of quadratic resisted projectile motion using the Lambert W function, *European Journal of Physics*, 35:055025–055032, 2014
4. J. Benacka. Solution to projectile motion with quadratic drag and graphing the trajectory in spreadsheets, *International Journal of Mathematical Education in Science and Technology*, 41:373–378, 2010.
5. J. Benacka. On high-altitude projectile motion, *Canadian Journal of Physics*, 89:1003–1008, 2011.
6. A. Bokhari. R. Belgacem, S. Kumar, D. Baleanu and S. Djilali, Projectile motion using three parameter Mittag-Leffler function calculus, *Mathematics and Computers in Simulation,* 195:22–30, 2022.
7. R.L. Burden and J.D. Faires. *Numerical Analysis*, Cengage Learning, 2016.
8. A. Ebaid. Analysis of projectile motion in view of the fractional calculus, *Applied Mathematical Modelling*, 35:1231–1239, 2011.
9. A. Ebaid, E.R. El-Zahar, A.F. Aljohani, B. Salah, M. Krid, J.T. Machado. Analysis of the two-dimensional fractional projectile motion in view of the experimental data, *Nonlinear Dynamics*, 97:711–1720, 2019.
10. G.R. Fowles and G.L. Cassiday. *Analytical Mechanics*, 7th Edition, Thomson Brooks/Cole, Belmont, 2005.
11. J.F. Gómez-Aguilar, J.J. Rosales-Garcìa, and J.J. Bernal-Alvarado. Fractional mechanical oscillators, *Revista Mexicana de Fisica*, 58:348–352, 2012.
12. J.C. Hayen. Projectile motion in a resistant medium. Part I: exact solution and properties, *International Journal of Non-Linear Mechanics*, 38:357–369, 2003.

13. J.C. Hayen. Projectile motion in a resistant medium. Part II: approximate solution and estimates, *International Journal of Non-Linear Mechanics*, 38:371–380, 2003.
14. R. Hilfer. *Applications of Fractional Calculus in Physics*, World Scientific, Singapore, 2000.
15. H. Hu, Y.P. Zhao, Y.J. Guo, M.Y. Zheng. Analysis of linear resisted projectile motion using the Lambert *W* function, *Acta Mechanica*, 223:441–447, 2012.
16. J.Juan Rosales Garcia, M.Guia Calderon, Juan Martinez Ortiz and Dumitru Baleanu. Motion of a particle in a resisting medium using fractional calculus approach, Proceedings of the Romanian Academy, 14:42–47, 2013.
17. C. Kittel, W. Knight, M. Ruderman, K. Helmholz. B. Moyer. *Berkeley Physics Course Mechanics*, vol. 1, McGraw Hill, New York, 1973.
18. A.K. Lazopoulos, D. Karaoulanis. Fractional Derivatives and Projectile Motion, *Axioms*, 10:297, 2021.
19. D.A. Morales. Exact expressions for the range and the optimal angle of a projectile with linear drag, *Canadian Journal of Physics*, 83:67–83, 2005.
20. K.S. Miller, and B. Ross. *An Introduction to the Fractional Calculus and Fractional Differential Equations*, Wiley, New York, 1993.
21. K.B. Oldham and J. Spanier. *The Fractional Calculus*, Academic Press, New York, 1974.
22. R. Ozarslan, E. Bas, D. Baleanu, B. Acay. Fractional physical problems including wind-influenced projectile motion with Mittag-Leffler kernel, *AIMS Mathematics*, 5:467–481, 2020.
23. I. Podlubny. *Fractional Differential Equations*, Academic Press, New York, 1999.
24. J.J. Rosales, M. Guia, F. Gomez, F. Aguilar, J. Martinez. Two-dimensional fractional projectile motion in a resisting medium, *Central European Journal of Physics*, 12:517–520, 2014.
25. S.G. Samko, A.A. Kilbas, and O.I. Marichev. *Fractional Integrals and Derivatives*, Theory and Applications, Gordon and Breach, Langhorne, PA, 1993.
26. S.T. Thornton and J.B. Marion. *Classical Dynamics of Particles and Systems*, 4th Edition, Saunders College Publications, New York, 1995.
27. P. Veeresha, E. Ilhan and H.M. Baskonus. Fractional approach for analysis of the model describing wind-influenced projectile motion, *Physica Scripta*, 96: 075209, 2021
28. K. Yabushita, M. Yamashita and K. Tsuboi. An analytic solution of projectile motion with the quadratic resistance law using the homotopy analysis method, *Journal of Physics A: Mathematical and Theoretical*, 40:8403–8416, 2007.

